

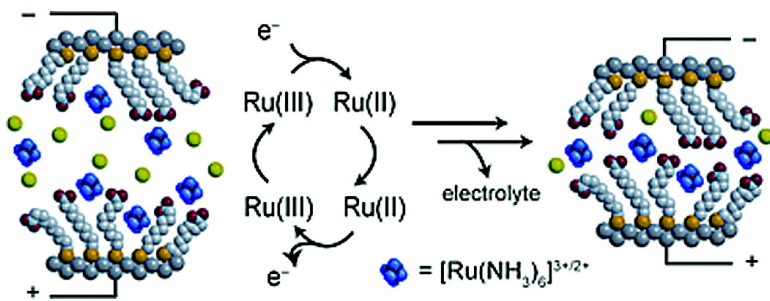
## Article

# Redox Site-Mediated Charge Transport in a Hg#SAM//Ru(NH)<sub>3</sub>//SAM#Hg Junction with a Dynamic Interelectrode Separation: Compatibility with Redox Cycling and Electron Hopping Mechanisms

Elizabeth Tran, Adam E. Cohen, Royce W. Murray, Maria A. Rampi, and George M. Whitesides

J. Am. Chem. Soc., 2009, 131 (6), 2141-2150 • DOI: 10.1021/ja804075y • Publication Date (Web): 22 January 2009

Downloaded from <http://pubs.acs.org> on February 12, 2009



## More About This Article

Additional resources and features associated with this article are available within the HTML version:

- Supporting Information
- Access to high resolution figures
- Links to articles and content related to this article
- Copyright permission to reproduce figures and/or text from this article

[View the Full Text HTML](#)

# Redox Site-Mediated Charge Transport in a Hg—SAM// Ru(NH<sub>3</sub>)<sub>6</sub><sup>3+/2+</sup>//SAM—Hg Junction with a Dynamic Interelectrode Separation: Compatibility with Redox Cycling and Electron Hopping Mechanisms

Elizabeth Tran,<sup>†</sup> Adam E. Cohen,<sup>†</sup> Royce W. Murray,<sup>§</sup> Maria A. Rampi,<sup>\*,‡</sup> and George M. Whitesides<sup>\*,†</sup>

Department of Chemistry and Chemical Biology, Harvard University, Cambridge, Massachusetts 02138; Dipartimento di Chimica, Università di Ferrara, 44100 Ferrara, Italy; and Kenan Laboratories of Chemistry, University of North Carolina, Chapel Hill, North Carolina 27510

Received May 30, 2008; E-mail: gwhitesides@gmwgroup.harvard.edu

**Abstract:** This paper describes the formation and electrical properties of a new Hg-based metal–molecules–metal junction that incorporates charged redox sites into the space between the electrodes. The junction is formed by bringing into contact two mercury-drop electrodes whose surfaces are covered by COO<sup>−</sup>-terminated self-assembled monolayers (SAMs) and immersed in a basic aqueous solution of Ru(NH<sub>3</sub>)<sub>6</sub>Cl<sub>3</sub>. The electrical behavior of the junction, which is contacted at its edges by aqueous electrolyte solution, has been characterized electrochemically. This characterization shows that current flowing through the junction on the initial potential cycles is dominated by a redox-cycling mechanism and that the rates of electron transport can be controlled by controlling the potentials of the mercury electrodes with respect to the redox potential of the Ru(NH<sub>3</sub>)<sub>6</sub><sup>3+/2+</sup> couple. On repeated cycling of the potential across the junction, the current across it increases by as much as a factor of 40, and this increase is accompanied by a large (>300 mV) negative shift in the formal potential for the reduction of Ru(NH<sub>3</sub>)<sub>6</sub><sup>3+</sup>. The most plausible rationalization of this behavior postulates a decrease in the size of the gap between the electrodes with cycling and a mechanism of conduction dominated by physical diffusion of Ru(NH<sub>3</sub>)<sub>6</sub><sup>3+/2+</sup> ions (at larger interelectrode spacing), with a possible contribution of electron hopping to charge transport (at smaller interelectrode spacing). In this rationalization, the negative shift in the formal potential plausibly reflects extrusion of the solution of electrolyte from the junction and an increase in the effective concentration of negatively charged species (surface-immobilized COO<sup>−</sup> groups) in the volume bounded by the electrodes. This junction has the characteristics required for use in screening and in exploratory work, involving nanogap electrochemical systems, and in mechanistic studies involving these systems. It does not have the stability needed for long-term technological applications.

## Introduction

This paper describes a new type of metal–molecules–metal junction containing redox-active centers. The junction (abbreviated Hg—SC<sub>10</sub>COO<sup>−</sup>//Ru(NH<sub>3</sub>)<sub>6</sub><sup>3+/2+</sup>//—OOCC<sub>10</sub>S—Hg) is formed from two mercury-drop electrodes whose surfaces are covered by COO<sup>−</sup>-terminated self-assembled monolayers (SAMs); these electrodes are brought into contact in a 1 mM solution of Ru(NH<sub>3</sub>)<sub>6</sub>Cl<sub>3</sub> in 0.1 M aqueous NaF at pH 9. This junction has been designed so that (i) redox centers trapped between the electrodes from a solution in electrolyte can transport charge between the electrodes by a redox cycling mechanism involving diffusion of Ru(NH<sub>3</sub>)<sub>6</sub><sup>3+/2+</sup> ions from one electrode to the other and (ii) the current flow across the junction can be controlled by controlling the potential of the electrodes with respect to the redox potential of the Ru(NH<sub>3</sub>)<sub>6</sub><sup>3+/2+</sup> ions.

An important goal in designing new molecule-based electronic devices is the control of the current flow between two terminals.

In molecular electronics, where the dielectric is composed of either single molecules or assemblies of molecules, the current flow between the two electrodes depends on the energy gap between the energy levels of the molecules and the Fermi levels of the electrodes.<sup>1</sup> Current flows when an orbital (usually the HOMO or LUMO) of the molecule falls between the Fermi levels of the electrodes. Thus, in designing molecular systems that can both mimic electronic functions and be utilized for fundamental studies of electron transfer processes, two features suggest promising directions for exploration: (i) the incorporation into these systems of redox-active molecules with well-defined, accessible, tunable energy states and (ii) the control of the potentials of the electrodes with respect to the redox potential of the molecules incorporated into the junction.

Early studies by Murray,<sup>2</sup> Wrighton,<sup>3</sup> and others<sup>4</sup> showed that when the electroactive species are confined between two closely spaced electrodes, a current mediated by these species flows when the potentials of the electrodes are controlled such that one donates electrons to these centers and the other accepts

<sup>†</sup> Harvard University.

<sup>‡</sup> Università di Ferrara.

<sup>§</sup> University of North Carolina.

(1) Aviram, A.; Ratner, M. A. *Chem. Phys. Lett.* **1974**, 29, 277–283.

them.<sup>2,5,6</sup> Under these conditions, two different mechanisms of charge transport may operate, depending on the mobility of the redox species in the interelectrode spacing and the rate of electron hopping between them.<sup>7,8</sup> (i) When the electroactive species can diffuse freely between the electrodes, the species generated at one electrode (the “generator” electrode) can diffuse to the second electrode (the “collector”).<sup>5,6,9</sup> The diffusion of the electroactive species between the generator and collector electrodes is called redox cycling.<sup>10</sup> (ii) When the mobility of the redox species is restricted (for example, by confinement in a polymer matrix sandwiched between the two electrodes),<sup>2</sup> charge flows from one electrode to the other by hopping of electrons between adjacent oxidized and reduced sites.

We have previously described a metal–molecules–metal junction that incorporates a bilayer of covalently linked, redox-active molecules between two metal electrodes.<sup>11</sup> By using liquid mercury as a “soft” metal contact,<sup>11–23</sup> it was possible to (i) bring two redox-active self-assembled monolayers (SAMs) into contact and (ii) form a junction in which the two electrodes can be individually contacted and separated from one another by a distance that is, in some circumstances, approximately equal to the thickness of the intervening SAMs. The junction consisted of two liquid mercury-drop electrodes whose surfaces were covered by SAMs terminated with covalently attached redox centers (R). Using a bipotentiostat to adjust the potentials of the electrodes to the electrochemical potential of the redox centers, we showed that this junction can be switched from an “off” to an “on” state and that charge transport through it is dominated by an electron-hopping mechanism across the interface between the two SAMs.

- (2) Pickup, P. G.; Murray, R. W. *J. Am. Chem. Soc.* **1983**, *105*, 4510–4514.
- (3) Kittlesen, G. P.; White, H. S.; Wrighton, M. S. *J. Am. Chem. Soc.* **1985**, *107*, 7373–7380.
- (4) Chidsey, C. E. D.; Murray, R. W. *Science* **1986**, *231*, 25–31.
- (5) Fosset, B.; Amatore, C. A.; Bartelt, J. E.; Michael, A. C.; Wightman, R. M. *Anal. Chem.* **1991**, *63*, 306–314.
- (6) Bard, A. J.; Crayston, J. A.; Kittlesen, G. P.; Shea, T. V.; Wrighton, M. S. *Anal. Chem.* **1986**, *58*, 2321–2331.
- (7) Blauch, D. N.; Saveant, J.-M. *J. Am. Chem. Soc.* **1992**, *114*, 3323–3332.
- (8) Blauch, D. N.; Saveant, J.-M. *J. Phys. Chem.* **1993**, *97*, 6444–6448.
- (9) Anderson, L. B.; Reiley, C. N. *J. Electroanal. Chem.* **1965**, *10*, 538–552.
- (10) Niwa, O.; Morita, M.; Tabei, H. *Anal. Chem.* **1990**, *62*, 447–452.
- (11) Tran, E.; Rampi, M. A.; Whitesides, G. M. *Angew. Chem., Int. Ed.* **2004**, *43*, 3835–3839.
- (12) Holmlin, R. E.; Haag, R.; Chabiny, M. L.; Ismagilov, R. F.; Cohen, A. E.; Terfort, A.; Rampi, M. A.; Whitesides, G. M. *J. Am. Chem. Soc.* **2001**, *123*, 5075–5085.
- (13) Holmlin, R. E.; Ismagilov, R. F.; Haag, R.; Mujica, V.; Ratner, M. A.; Rampi, M. A.; Whitesides, G. M. *Angew. Chem., Int. Ed.* **2001**, *40*, 2316–2320.
- (14) Slowinski, K.; Chamberlain, R. V.; Bilewicz, R.; Majda, M. *J. Am. Chem. Soc.* **1996**, *118*, 4709–4710.
- (15) Slowinski, K.; Chamberlain, R. V.; Miller, C. J.; Majda, M. *J. Am. Chem. Soc.* **1997**, *119*, 11910–11919.
- (16) Slowinski, K.; Fong, H. K. Y.; Majda, M. *J. Am. Chem. Soc.* **1999**, *121*, 7257–7261.
- (17) Slowinski, K.; Majda, M. *J. Electroanal. Chem.* **2000**, *491*, 139–147.
- (18) Slowinski, K.; Slowinska, K. U.; Majda, M. *J. Phys. Chem. B* **1999**, *103*, 8544–8551.
- (19) Chabiny, M. L.; Chen, X.; Holmlin, R. E.; Jacobs, H.; Skulason, H.; Frisbie, C. D.; Mujica, V.; Ratner, M. A.; Rampi, M. A.; Whitesides, G. M. *J. Am. Chem. Soc.* **2002**, *124*, 11730–11736.
- (20) Liu, Y. J.; Yu, H. Z. *Chem. Phys. Chem.* **2002**, *3*, 799–802.
- (21) Liu, Y. J.; Yu, H. Z. *J. Electrochem. Soc.* **2003**, *150*, G861–G865.
- (22) Selzer, Y.; Salomon, A.; Cahen, D. *J. Phys. Chem. B* **2002**, *106*, 10432–10439.
- (23) York, R. L.; Nguyen, P. T.; Slowinski, K. *J. Am. Chem. Soc.* **2003**, *125*, 5948–5953.

Here, we describe the fabrication and characterization of a simpler, and chemically more flexible, Hg-based metal–molecules–metal junction containing soluble (i.e., not covalently immobilized) redox centers. Our objective in this work was to demonstrate that this junction can (i) efficiently transport charge between two mercury electrodes separated by two contacting SAMs by a redox cycling mechanism and (ii) allow current flow to be controlled electrochemically using the potentials of the mercury electrodes with respect to an external reference electrode.

The junction consists of two mercury-drop electrodes whose surfaces support nonelectroactive SAMs carrying negatively charged terminating groups; these fixed charges allow an oppositely (positively) charged redox center, originally present in a solution of electrolyte in which the mercury-drop electrodes are immersed, to be trapped electrostatically between the two electrodes. We chose  $\text{COO}^-$ -terminated SAMs formed from 11-mercaptopundecanoic acid (abbreviated  $\text{HSC}_{10}\text{COOH}$ ) because they are electrochemically inactive, easy to prepare from commercial precursors, and stable to electrochemical measurements over the potential range of mercury. Because they have a negatively charged surface and a disordered structure,<sup>24–26</sup> we expected these SAMs both to attract electroactive cations from a contacting solution and to allow these ions access to the surface of the mercury electrodes via permeable sites (defects, and disordered, liquidlike regions) in the SAMs.<sup>25</sup> We chose  $\text{Ru}(\text{NH}_3)_6\text{Cl}_3$  as the redox probe because it undergoes a rapid, outer-sphere, chemically reversible one-electron redox reaction and because both the oxidized and reduced forms of the ruthenium complex,  $\text{Ru}(\text{NH}_3)_6^{3+}$  and  $\text{Ru}(\text{NH}_3)_6^{2+}$ , are positively charged.<sup>27</sup>

The SAMs sandwiched between the mercury electrodes in this new junction (henceforth abbreviated  $\text{Hg}-\text{SC}_{10}\text{COO}^-/\text{Ru}(\text{NH}_3)_6^{3+/2+}/\text{OOCC}_{10}\text{S}-\text{Hg}$ ) thus play the dual role of (i) acting as spacers between the electrodes and thus preventing the Hg drops from merging with one another and (ii) acting as supporting matrices—essentially monolayer ion-exchange membranes—that attract  $\text{Ru}(\text{NH}_3)_6^{3+}$  and  $\text{Ru}(\text{NH}_3)_6^{2+}$  ions. Here, we demonstrate that, by placing the junction together with a  $\text{Ag}/\text{AgCl}$  reference electrode and a platinum counter electrode, in an aqueous electrolyte solution in an electrochemical cell, and by using a bipotentiostat, it is possible to control the potentials of the two mercury electrodes independently with respect to that of the reference electrode and therefore to control the potentials of the mercury electrodes with respect to the formal potential of the ruthenium centers. We have explored the effect of controlling these potentials in two types of generation-collection<sup>6</sup> experiments. In one experiment, the potential of one electrode is kept constant while that of the second electrode is varied. In the second experiment, the potentials of both electrodes are changed with respect to a reference electrode while maintaining a constant difference between them. Figure 1 shows the junction schematically and the associated electrochemical system.

For both experiments, the results show that the current passes across the junction, via the ruthenium sites, only when the potentials of the mercury electrodes are set so as to reduce

- (24) Finkle, H. O. In *Electroanalytical Chemistry*; Bard, A. J., Rubinstein, I., Eds.; Marcel Dekker: New York, 1996; Vol. 19, pp 109–335.
- (25) Chidsey, C. E. D.; Loiacono, D. N. *Langmuir* **1990**, *6*, 682–691.
- (26) Mendes, R. K.; Freire, R. S.; Fonseca, C. P.; Neves, S.; Kubota, L. T. *J. Braz. Chem. Soc.* **2004**, *15*, 849–855.
- (27) Tsou, Y.-M.; Anson, F. C. *J. Electrochem. Soc.* **1984**, *131*, 595–601.

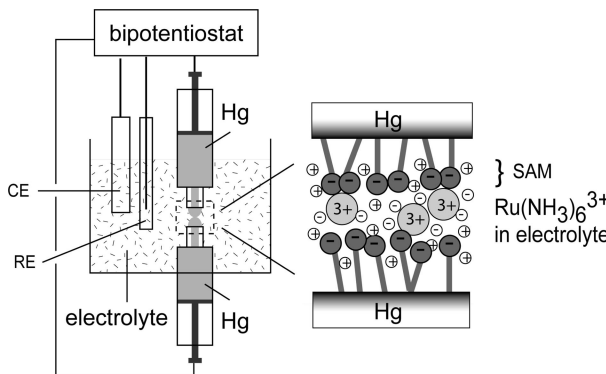


**Figure 1.** Schematic representation of the  $\text{Hg}-\text{SC}_{10}\text{COO}^-/\text{Ru}(\text{NH}_3)_6^{3+/2+}/-\text{OOCC}_{10}\text{S}-\text{Hg}$  junction and the electrochemical cell arrangements used in this work. CE = Pt gauze counter electrode. RE = Ag/AgCl reference electrode.

$\text{Ru}(\text{NH}_3)_6^{3+}$  to  $\text{Ru}(\text{NH}_3)_6^{2+}$  at one electrode and to oxidize  $\text{Ru}(\text{NH}_3)_6^{2+}$  to  $\text{Ru}(\text{NH}_3)_6^{3+}$  at the other. As the number of cyclic potential sweeps (from two to about eight) increases, three events occur: (i) the current across the junction increases by more than a factor of 40, (ii) the efficiency of collection, defined as the ratio of the collector current to the generator current, approaches unity (typically 0.93–0.98), and (iii) the formal potential (represented by  $E_{1/2}^{\text{f}}$ ) of the ruthenium species inside the junction shifts negatively by at least 262 mV from the value measured at a single mercury electrode in contact with bulk solution. We hypothesize that the marked increase in current is due to a decrease in the interelectrode spacing that occurs with continuous, repeated cycling of the potential across the junction. A decrease in interelectrode spacing, in principle, can be caused by a number of factors, including extrusion of the solvent, and/or tilting, compression, or extension of the SAMs under electrostrictive pressure.<sup>22,28</sup> In this paper, we discuss factors that might contribute to the decrease in interelectrode spacing. We also discuss the possibility that, in the confined space between the two SAMs, as the interelectrode gap become smaller and smaller, a competitive mechanism involving electron hopping between concentrated, and perhaps electrostatically immobilized,  $\text{Ru}(\text{NH}_3)_6^{3+/2+}$  ions can also operate.

## Experimental Section

**Chemicals.** All chemicals were used as received from commercial sources unless stated otherwise. Ruthenium hexaammine ( $\text{Ru}(\text{NH}_3)_6\text{Cl}_3$ ) and  $\text{NaClO}_4$  (98–102%) were purchased from Alfa Aesar. Electronic grade mercury (99.9999%),  $\text{Na}_2\text{SO}_4$  (99.99%),  $\text{NaF}$  (99.99%),  $\text{NaNO}_3$  (99.995%), and 11-mercaptopoundecanoic acid (recrystallized from ethanol) were purchased from Aldrich. **CAUTION:** Mercury is highly toxic if swallowed or if its vapors are inhaled. Thiol deposition solutions were prepared with ethanol (200 proof) from Pharmaco. Electrolyte solutions were prepared with deionized water from a Millipore purification system and adjusted to pH 9 with either aqueous  $\text{NaOH}$ ,  $\text{KOH}$ , or  $\text{LiOH}$ . For 0.1 M  $\text{Na}_2\text{SO}_4$  solutions with lower pH, concentrated sulfuric acid was used.

**Electrochemical Apparatus and Measurements.** All electrochemical measurements were performed at ambient temperatures in 10-mL electrolyte solutions that had been purged with argon for 10 min. The measurements were carried out using a Pine Model AFCBP1 bipotentiostat, a platinum gauze counterelectrode (Alfa

Aesar), and a Ag/AgCl reference electrode (BAS). For conventional cyclic voltammetry, a three-electrode-single-compartment cell was used, with a hanging mercury-drop electrode (HMDE) serving as the working electrode. The HMDE was prepared by extruding a drop of liquid mercury from a 1-mL gastight Hamilton syringe and exposing it to an aerated ethanolic solution of thiol. A tungsten wire protruding from the Teflon tip of the syringe plunger provided an electrical connection between the mercury electrode and the bipotentiostat. The syringe was attached to a micromanipulator, which was used to immerse and remove the mercury drop from solutions of electrolyte and from solutions used for rinsing after self-assembly. For generation-collection measurements, two HMDEs were employed: one pointing downward and attached to the micromanipulator and a second pointing upward and situated in the center of a custom-built cell (Figure 1). The cell was a glass cylinder with an open top and a base having a hole of the same diameter as that of the mercury-containing syringe in the center. To seal the gap between the syringe and the cell at the hole, epoxy glue was used.

**Monolayers and Junctions.** Monolayers of  $\text{SC}_{10}\text{COOH}$  were prepared by dispensing 2–3 drops of a 1 mM solution of 11-mercaptopoundecanoic acid in ethanol on top of a freshly extruded drop of liquid mercury. After 3 min of incubation, the SAM-coated drop(s) of mercury were rinsed successively with ethanol and water. In order not to disturb the SAMs, the rinsing was carried out by filling the cell with ethanol by syringe until the ethanol covered the HMDEs. After about 30 s, the ethanol was removed slowly by syringe and the process was repeated for water to yield the SAM-covered mercury-drop electrodes used for assembling the  $\text{Hg}-\text{SC}_{10}\text{COO}^-/\text{Ru}(\text{NH}_3)_6^{3+/2+}/-\text{OOCC}_{10}\text{S}-\text{Hg}$  junction.

To assemble the  $\text{Hg}-\text{SC}_{10}\text{COO}^-/\text{Ru}(\text{NH}_3)_6^{3+/2+}/-\text{OOCC}_{10}\text{S}-\text{Hg}$  junction, the cell was next equipped with a Pt gauze counterelectrode and a Ag/AgCl reference electrode and filled with a pH 9 electrolyte solution containing 1 mM ruthenium hexaammine. The micromanipulator attached to the HMDE on top was then used to position it vertically and coaxially with the HMDE on the bottom as shown in Figure 1. The Ru-containing electrolyte solution could subsequently be replaced with a Ru-free electrolyte solution.

## Results and Discussion

This section begins with a description of the formation and characterization of COOH-terminated SAMs formed by chemisorption of 11-mercaptopoundecanoic acid on mercury, with emphasis on the influence of pH and composition of the electrolyte solution on the electrochemical redox behavior of  $\text{Ru}(\text{NH}_3)_6^{3+}$  at this electrode. A description of the  $\text{Hg}-\text{SC}_{10}\text{COO}^-/\text{Ru}(\text{NH}_3)_6^{3+/2+}/-\text{OOCC}_{10}\text{S}-\text{Hg}$  junction and studies of charge transport across it follow.

**Preparation and Characterization of SAMs of  $\text{SC}_{10}\text{COOH}$  and  $\text{SC}_{10}\text{COO}^-$  on Mercury Electrodes.** SAMs formed from alkanethiols by chemisorption on mercury have been studied extensively.<sup>29–32</sup> We prepared mercury electrodes modified with COOH-terminated SAMs using a procedure similar to that described previously.<sup>12,13,33</sup> We extruded drops of mercury (~1–2 mm in diameter) from a 1-mL, gastight syringe into a 1-mM solution of  $\text{HSC}_{10}\text{COOH}$  in ethanol. After removing the drop electrodes from the thiol-containing solution, we rinsed

- (29) Ocko, B. M.; Kraack, H.; Pershan, P. S.; Sloutskin, E.; Tamam, L.; Deutsch, M. *Phys. Rev. Lett.* **2005**, 94, 017802/1–017802/4.
- (30) Tamam, L.; Kraack, H.; Sloutskin, E.; Ocko, B. M.; Pershan, P. S.; Ulman, A.; Deutsch, M. *J. Phys. Chem. B* **2005**, 109, 12534–12543.
- (31) Magnussen, O. M.; Ocko, B. M.; Deutsch, M.; Regan, M. J.; Pershan, P. S.; Abernathy, D.; Gurebel, G.; Legrand, J.-F. *Nature* **1996**, 384, 250–252.
- (32) Deutsch, M.; Magnussen, O. M.; Ocko, B. M.; Regan, M. J.; Pershan, P. S. *Thin Films* **1998**, 24, 179–203.
- (33) Haag, R.; Rampi, M. A.; Holmlin, R. E.; Whitesides, G. M. *J. Am. Chem. Soc.* **1999**, 121, 7895–7906.

(28) Cui, X. D.; Primak, A.; Zarate, X.; Tomfohr, J.; Sankey, O. F.; Moore, A. L.; Moore, T. A.; Gust, D.; Nagahara, L. A.; Lindsay, S. M. *J. Phys. Chem. B* **2002**, 106, 8609–8614.

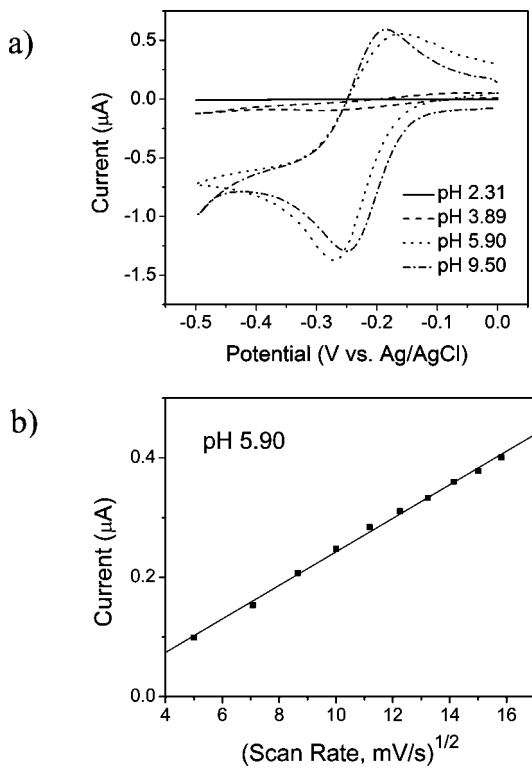


**Figure 2.** Cyclic voltammograms for 1 mM  $\text{Ru}(\text{NH}_3)_6^{3+}$  in 0.1 M aqueous  $\text{Na}_2\text{SO}_4$  at different values of pH on  $\text{SC}_{10}\text{COOH}$ -covered mercury electrodes. The scan rate was 50 mV/s. The surface area of the mercury electrodes was  $\sim 6 \text{ mm}^2$  throughout this set of experiments.

them (with their coating of SAM) by successive immersions in ethanol and in deionized water, for 10 s each. We assessed the permeability of the SAMs and their ability to attract ionic redox molecules, using cyclic voltammetry. For the self-assembly and rinsing steps, we clamped the mercury-containing syringe in a fixed position and used an adjustable stage to raise and lower the electrochemical cell containing the appropriate solution; this procedure minimized but did not eliminate mechanical disturbance (and possible disruption) of the surface of the mercury drops and of the SAMs. It also avoided inadvertent dislodging of the mercury drop from the syringe tip (Figure 1a). Because this SAM is relatively fluid (since it has a short- $(\text{CH}_2)_{10}$ -hydrophobic chain), we believe that lateral diffusion heals cracks or breaks caused by vibration of the drop or by liquid shear. For each solution, we used a different cell so as to minimize contamination. This procedure was also used to replace the rinsing solutions with electrolyte.

**Permeability of the  $\text{COO}^-$ -Terminated SAMs.** We measured the permeability of the SAMs to  $\text{Ru}(\text{NH}_3)_6^{3+}$  as a function of the pH of the electrolyte solution, at a single mercury electrode. We expected the pH of the electrolyte to influence the permeability of the SAMs in a fashion analogous to that described previously for SAMs of  $\text{SC}_{10}\text{COOH}$  on gold substrates;<sup>24–26</sup> that is, we expected the SAMs to be impermeable when the COOH groups were protonated and permeable when the COOH groups were ionized. Figure 2 shows results of immersing the SAM-covered mercury electrodes ( $\sim 1 \text{ mm}$  in diameter) in 0.1 M aqueous  $\text{Na}_2\text{SO}_4$  containing 1 mM  $\text{Ru}(\text{NH}_3)_6^{3+}$  at four different values of pH. Cyclic voltammetry (Figure 2a) showed that at a value of pH less than 4, where the terminal COOH groups are protonated and thus electrically neutral, the current across the junction is negligible and

independent of potential, as expected for an impermeable dielectric monolayer. At pHs 5 and 9, the cyclic voltammograms are essentially indistinguishable and exhibit a well-defined redox wave for the reversible reduction of  $\text{Ru}(\text{NH}_3)_6^{3+}$  at  $E^\circ$  (taken as the average of the anodic and cathodic peak potentials) =  $-0.21 \text{ V}$  versus Ag/AgCl. For both cyclic voltammograms, the peak splitting of  $\sim 86 \text{ mV}$  indicates quasireversible behavior. Because the redox wave appears at about the same potential as that observed at a bare mercury electrode and because the anodic currents are proportional to the square root of scan rate (Figure 2b), we conclude that, at a value of pH above 5, the SAMs are no longer blocking (although they may modestly retard the electron transfer rates) and that reduction of  $\text{Ru}(\text{NH}_3)_6^{3+}$  occurs at defect sites in the SAMs via a diffusion-controlled process. For comparison, the reported  $pK_a$  values for adsorbed 11-mercaptopundecanoic acid on gold vary between 5.5 and 8.5.<sup>34,35</sup> Thus, following previously reported results,<sup>25</sup> we attribute the nonblocking behavior of the SAMs to a disordered structure, presumably reflecting electrostatic repulsion among the closely packed, terminal  $\text{COO}^-$  groups.<sup>36–43</sup>

#### Interactions of the $\text{COO}^-$ -Terminated SAMs with $\text{Ru}(\text{NH}_3)_6^{3+2+}$ .

To study the interactions of the  $\text{COO}^-$ -terminated SAMs with the  $\text{Ru}(\text{NH}_3)_6^{3+2+}$  ions at the SAM/electrolyte interface, we used the same SAM-coated mercury electrode to examine the effects of  $\text{Li}_2\text{SO}_4$ ,  $\text{Na}_2\text{SO}_4$ ,  $\text{K}_2\text{SO}_4$ , and  $\text{NaF}$  as electrolytes on the electrochemical behavior of the  $\text{Ru}(\text{NH}_3)_6^{3+2+}$  system. Figure 3a shows that the choice of cation of the electrolyte has little influence on the magnitude or the potential of the redox wave and hence suggests that these monovalent cations present in the electrolyte do not compete with the  $\text{Ru}(\text{NH}_3)_6^{3+}$  ion for interaction with  $\text{COO}^-$  moieties of the monolayers. In contrast, increasing the concentration of the electrolyte by 10-fold leads to a negative shift in  $E^\circ$  from  $-0.14$  to  $-0.18 \text{ V}$  versus Ag/AgCl for the  $\text{Ru}(\text{NH}_3)_6^{3+2+}$  couple and a small (12%) reduction in the peak currents (Figure 3b). We attribute the reduction in peak currents to a corresponding decrease in concentration of  $\text{Ru}(\text{NH}_3)_6^{3+2+}$  at the surface of the SAM or perhaps to more subtle effects due to the small changes in interfacial viscosity or structure of the SAM and its contacting solution. The negative shift in  $E^\circ$ , on the other hand, is in the direction expected if reduction of  $\text{Ru}(\text{NH}_3)_6^{3+}$  were to become energetically more difficult and may be due to the decrease in ionic strength, which in turn would lead to an increase in the Donnan potential at the monolayer/solution interface and an increase in the solvation of the ruthenium species by the anions of the electrolyte.

Comparison of Figure 3a with Figure 3b shows that decreasing the negative charge of the anion of the electrolyte by one unit (i.e., from  $\text{SO}_4^{2-}$  to  $\text{F}^-$ ) leads to a positive shift in  $E^\circ$  of

- (34) Smalley, J. F.; Chalfant, K.; Feldberg, S. W.; Nahir, T. M.; Bowden, E. F. *J. Phys. Chem. B* **1999**, *103*, 1676–1685.
- (35) Kakiuchi, T.; Iida, M.; Imabayashi, S.; Niki, K. *Langmuir* **2000**, *16*, 5397–5401.
- (36) Ganesan, P. G.; Singh, A. P.; Ramanath, G. *Appl. Phys. Lett.* **2004**, *85*, 579–581.
- (37) Calvente, J. J.; Lopez-Perez, G.; Ramirez, P.; Fernandez, H.; Zon, M. A.; Mulder, W. H.; Andreu, R. *J. Am. Chem. Soc.* **2005**, *127*, 6476–6486.
- (38) Lee, T. R.; Carey, R. I.; Biebuyck, H. A.; Whitesides, G. M. *Langmuir* **1994**, *10*, 741–749.
- (39) Creager, S. E.; Clarke, J. *Langmuir* **1994**, *10*, 3675–3683.
- (40) White, H. S.; Peterson, J. D.; Cui, Q.; Stevenson, K. J. *J. Phys. Chem. B* **1998**, *102*, 2930–2934.
- (41) Shimazu, K.; Teranishi, T.; Sugihara, K.; Uosaki, K. *Chem. Lett.* **1998**, *7*, 669–670.
- (42) Dai, Z.; Ju, H. *Phys. Chem. Chem. Phys.* **2001**, *3*, 3769–3773.
- (43) Aoki, K.; Kakiuchi, T. *J. Electroanal. Chem.* **1998**, *452*, 187–192.

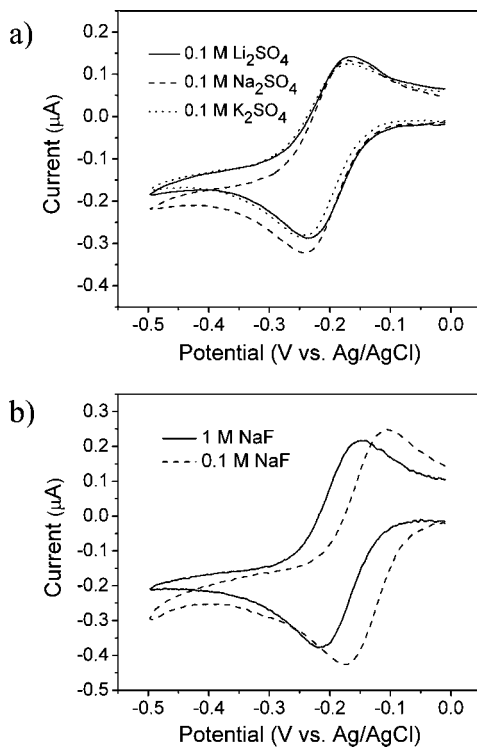


**Figure 3.** Cyclic voltammograms of  $\text{SC}_{10}\text{COOH}$ -covered mercury electrodes in 1 mM  $\text{Ru}(\text{NH}_3)_6^{3+}$  as a function of (a) the cations and (b) the anion and concentration of the electrolyte. The scan rate was 50 mV/s. The surface area of the mercury electrodes was  $\sim 3 \text{ mm}^2$  throughout this set of experiments.

about 70 mV for the  $\text{Ru}(\text{NH}_3)_6^{3+/2+}$  couple. This positive shift in  $E^\circ$  is in the direction expected if the reduction of  $\text{Ru}(\text{NH}_3)_6^{3+}$  was to become energetically more favorable and suggests that the electrostatic interaction between  $\text{F}^-$  and the Ru(III) oxidation state of the ruthenium complex (as opposed to the Ru(II) reduction state) is weaker than for  $\text{SO}_4^{2-}$ . The variation of  $E^\circ$  with ionic strength in this case (i.e., from 0.3 in 0.1 M  $\text{Na}_2\text{SO}_4$  to 0.1 in 0.1 M NaF) is likely small, since changing the ionic strength of the electrolyte by 10-fold as discussed above leads to a shift in  $E^\circ$  of only 20 mV.

To confirm that the interaction between the  $\text{Ru}(\text{NH}_3)_6^{3+}$  complex and the  $\text{COO}^-$  moieties of the SAMs is a weak ionic association, we transferred (without washing) an electrode that had been subjected to three or four cycles of potential (between  $-0.5$  and  $0$  V, in 0.1 M NaF (pH 9) containing 1 mM  $\text{Ru}(\text{NH}_3)_6^{3+}$ ) to a NaF solution (pH 9) that was free of the ruthenium species. We carried out this transfer in two steps: we first lowered the electrochemical cell to separate the electrode from the electrolyte solution and then raised a new electrochemical cell containing a ruthenium-free electrolyte to reimmerse the electrode. On the initial scan (taken 3 s after reimersion), the redox wave in the absence of added  $\text{Ru}(\text{NH}_3)_6^{3+}$  was similar to that observed in solutions containing this ion. Repeated cycling (two or three cycles) however led to a progressive decrease in both the cathodic and anodic currents. It is thus clear that the  $\text{Ru}(\text{NH}_3)_6^{3+}$  ion is not held irreversibly to the surface of the SAM and that it can exchange with electrolyte ions and diffuse into the solution.

**Assembly of the  $\text{Hg}-\text{SC}_{10}\text{COO}^-/\text{Ru}(\text{NH}_3)_6^{3+/2+}/-\text{OOCC}_{10}\text{S}-\text{Hg Junction}$ .** To assemble a mercury-drop junction that incorporates a facing bilayer of  $\text{SC}_{10}\text{COO}^-$  molecules and allows a thin film of  $\text{Ru}(\text{NH}_3)_6^{3+}$  solution to be trapped between the

electrodes, we used a single-compartment electrochemical cell equipped with two mercury-containing syringes (Figure 1). We first formed SAMs of  $\text{SC}_{10}\text{COOH}$  on freshly generated mercury-drop electrodes from a 1-mM solution of  $\text{HSC}_{10}\text{COOH}$  in ethanol. After rinsing the SAMs successively with ethanol and deionized water as described previously, we used a disposable polyethylene syringe that was connected to a needle with polyethylene tubing ( $\sim 0.45$  mm in diameter and 1 in. in length) attached to it to fill the electrochemical cell with a deoxygenated solution of electrolyte (either 0.1 M NaF or  $\text{Na}_2\text{SO}_4$  in water) that had been adjusted to pH 9 with aqueous NaOH and that contained 1 mM  $\text{Ru}(\text{NH}_3)_6\text{Cl}_3$  (see Experimental Section). We then measured CVs for each electrode separately, to ensure that each gave similar responses (as they must, barring from contamination or artifacts, since they were exposed to the same solution). Next, we brought the SAM-coated mercury electrodes into contact in the presence of this electrolyte using a micro-manipulator. We then measured the area of contact ( $\sim 0.8 \text{ mm}^2$ ) between the two mercury drops by visual comparison (at 5 $\times$  magnification) of the diameter of the  $\text{Hg}-\text{Hg}$  contact area relative to the known diameter (1 mm) of the glass barrels from which the mercury drops were extruded.

The use of electrolyte solutions at pH 9 proved critical to our study. At this pH, the negatively charged SAMs interacted electrostatically with the positively charged  $\text{Ru}(\text{NH}_3)_6^{3+/2+}$  species, and the negative charges on the SAMs prevented coalescence of the mercury-drop electrodes, allowed the SAMs to be permeable to the ruthenium species, and permitted facile electron transfers of the  $\text{Ru}(\text{NH}_3)_6^{3+/2+}$  couple. We emphasize<sup>44</sup> that the presence of the  $\text{COO}^-$  groups was necessary for the stability of the junction.

**Electrochemical Measurements.** A four-electrode electrochemical system was used to investigate the redox behavior of  $\text{Ru}(\text{NH}_3)_6^{3+/2+}$  in the  $\text{Hg}-\text{SC}_{10}\text{COO}^-/\text{Ru}(\text{NH}_3)_6^{3+/2+}/-\text{OOCC}_{10}\text{S}-\text{Hg}$  junction. The potentials of the two mercury-drop electrodes could be controlled independently, relative to that of the Ag/AgCl reference electrode, with a bipotentiostat (Figure 1). The potentials were controlled such that one electrode acted as an electron donor to  $\text{Ru}(\text{NH}_3)_6^{3+}$  and the other acted as an electron acceptor from  $\text{Ru}(\text{NH}_3)_6^{2+}$ . Two types of generation-collection experiments were carried out, which we termed “A<sup>Gen</sup>” and “B<sup>Both</sup>”, for brevity. In experiment A<sup>Gen</sup>, we kept the potential of one electrode (the “collector” electrode) constant and changed that of the second electrode (the “generator”). In experiment B<sup>Both</sup>, we varied the potentials of both electrodes simultaneously while maintaining a constant difference in potential between them. The  $\text{Ru}(\text{NH}_3)_6^{3+}$ -containing electrolyte (pH 9) used to make the junction could continue to surround its edges in these experiments, or it could be replaced by a Ru-free but otherwise indistinguishable solution of electrolyte.

**Generation-Collection Experiment A<sup>Gen</sup>. Scanning the Potential of One Mercury Electrode.** The generator electrode was swept toward negative potentials, past  $E^\circ$  ( $-0.21$  V) for the  $\text{Ru}(\text{NH}_3)_6^{3+} \rightarrow \text{Ru}(\text{NH}_3)_6^{2+}$  reaction and back again while the potential of the collector electrode was held at  $+0.10$  V versus Ag/AgCl, so that the  $\text{Ru}(\text{NH}_3)_6^{2+}$  generated was oxidized to  $\text{Ru}(\text{NH}_3)_6^{3+}$  (Figure 4). The generator electrode was typically first cycled briefly (2–4 cycles) in the 1 mM  $\text{Ru}(\text{NH}_3)_6^{3+}$ ; this

(44) Although mechanically stable junctions could be formed in electrolytes at pH  $< 4$ , they were not stable with respect to coalescence of the two mercury drops during electrochemical measurements.

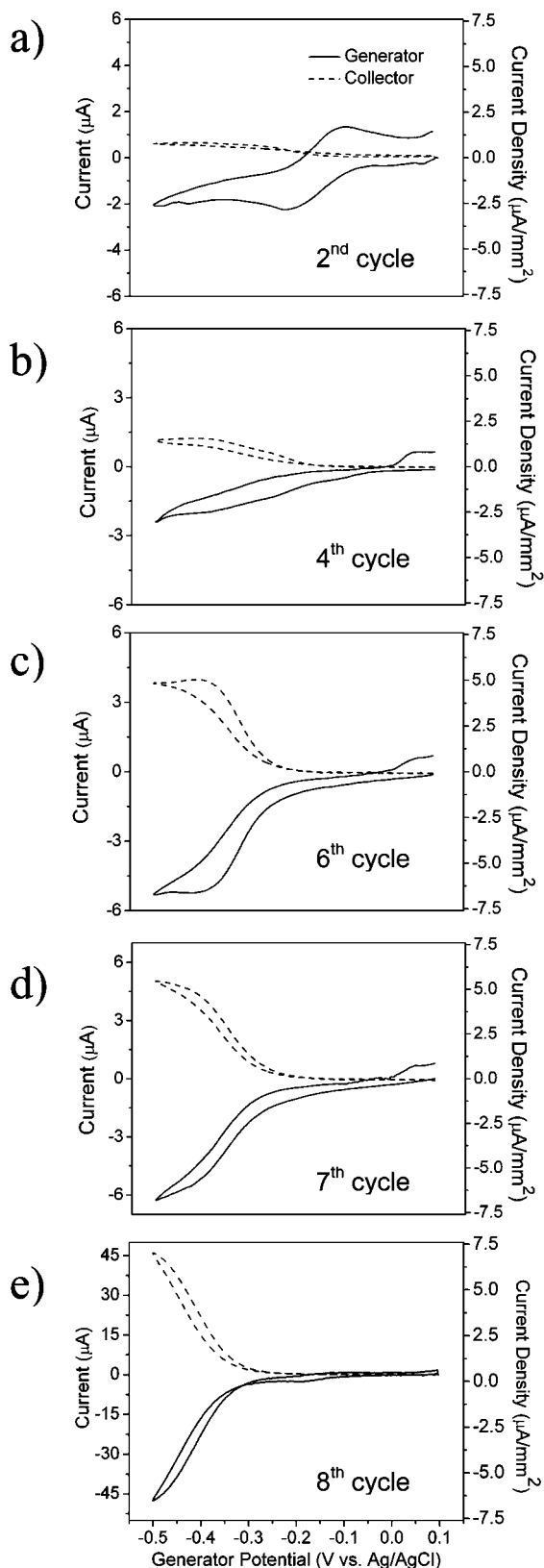


**Figure 4.** Generation-collection voltammograms of 1 mM  $\text{Ru}(\text{NH}_3)_6^{3+}$  in a  $\text{Hg}-\text{SC}_{10}\text{COO}^-/\text{Ru}(\text{NH}_3)_6^{3+/2+}/-\text{OOCC}_{10}\text{S}-\text{Hg}$  junction in 0.1 M NaF at pH 9. The collector potential was held at +0.10 V, and the generator potential was cycled between +0.10 and -0.50 V at a scan rate of 50 mV/s (solid line, generator current; dashed line, collector current). The area of the junction was ca. 0.79 mm<sup>2</sup> throughout this set of experiments.

initial set of scans made it possible for us to assess the quality of the junction. Under these conditions, the first few potential

scans (Figure 4a) produced a reversible wave at the generator electrode that was essentially indistinguishable from that observed for the same junction (not shown) when the generator and collector electrodes were not in contact and the collector electrode was disconnected from the bipotentiostat. For example, the charge under the voltammetric waves at the generator electrode before and after the formation of the junction and the separations between the cathodic and anodic peaks were about the same. This behavior is not unexpected, since the surfaces of the mercury drops not in the junction remain exposed to the  $\text{Ru}(\text{NH}_3)_6^{3+}$  solution. It also suggests that the junction is initially laterally open and porous (that is, ions can diffuse in and out of the space between the mercury drops from the surrounding solution of electrolyte).

After 2–4 potential cycles, the electrolyte solution containing  $\text{Ru}(\text{NH}_3)_6^{3+}$  was carefully removed by syringe in a way that did not destroy the junction and then replaced with a pure electrolyte solution at the same pH (details are in the Experimental Section). With repeated cycling of the potential, the current–voltage curve at the generator electrode changed significantly (Figure 4b–e). The current initially increased slowly and then typically (but not always, as described below) became sigmoidal and increased rapidly with each successive sweep cycle until a steady-state current–voltage curve (i.e., the currents of the forward and reverse scans were about the same and no longer changed with cycling of the potential) was obtained. We observed a similar behavior at the collector electrode; that is, the current increased slowly in the first cycles and then rapidly and finally reached a steady state.

We propose that the gradual increase in current at the collector electrode is due mainly to a change from a Ru(III) solution to a mixture of Ru(III/II), which in turn requires a change in the concentration of the compensating counterions ( $\text{Cl}^-$  and  $\text{F}^-$ ). The latter may occur as a result of electrolyte anions being gradually ejected from the thin layer of solvent between the mercury surfaces (or cations being brought into this layer). This behavior, where a significant current can also be observed at the collector electrode, is strong evidence that  $\text{Ru}(\text{NH}_3)_6^{3+/2+}$  is trapped inside the junction and that the two SAM-covered mercury electrodes are sufficiently close that redox cycling occurs.

A similar steady-state current response was also observed when the electrolyte containing  $\text{Ru}(\text{NH}_3)_6^{3+}$  was not removed from the electrochemical cell. The currents that flow on the sides of the mercury-drop electrodes simply become insignificant compared to the growing currents from the junction. This last result is important because it confirms that the marked increase in current with the number of cycles of potential is due primarily to the presence of ruthenium ions inside the  $\text{Hg}-\text{SC}_{10}\text{COO}^-/\text{Ru}(\text{NH}_3)_6^{3+/2+}/-\text{OOCC}_{10}\text{S}-\text{Hg}$  junction.

In general, the number of cycles required for the currents to approach steady-state behavior ranged from 5 to 15; in some cases (see below), however, such behavior simply could not be reached by increasing the number of potential cycles alone. An alternative approach for achieving steady-state currents involved two steps. In the first step, we decreased the separation between the two syringes supporting the mercury drops so that the pressure on the junction, the area of the junction, and the distortion of the two SAM-covered mercury drops increased slightly. The potential of the generator electrode was then cycled 1–2 times. This two-step procedure was then repeated until a well-defined steady-state voltammogram appeared. The observation that this two-step procedure was sometimes required for

production of steady-state behavior of the type shown in Figure 4e suggests that time per se does not determine the behavior of the system.

The two-step approach described above however does not always lead to steady-state currents. It is apparently possible not to achieve steady-state currents even when the two mercury-containing syringes are sufficiently close to one another that their mercury drops are distorted from their noncontact spherical shape by the interaction (“contact”) between them. The inability of the junction to reach the configuration (geometry and composition) required to produce steady-state behavior could be due to the presence of contaminants, such as dust particles or oxides, on the mercury surface. Finally, we note that the dynamics of the thinning of the electrolyte layer (see below) are complex and still not completely defined in our experiments.

The increase in current was accompanied by a negative shift of the half-wave (half-maximum) potential  $E_{1/2}$  relative to  $E^\circ$  for the  $\text{Ru}(\text{NH}_3)_6^{3+} \rightleftharpoons \text{Ru}(\text{NH}_3)_6^{2+}$  reaction and an increase in the collection efficiency (i.e., the ratio of the current at the collector electrode to that at the generator electrode). For example, when  $i_{\text{lim}}(\text{collector}) = 0.95 \mu\text{A}$ ,  $E_{1/2}$  was  $-0.29 \text{ V}$ , and the collection efficiency was 0.44, but when  $i_{\text{lim}} = 5.00 \mu\text{A}$ ,  $E_{1/2}$  was  $-0.35 \text{ V}$ , and the collection efficiency was 0.81. The value of  $E_{1/2}$  corresponds to the formal potential for reduction of  $\text{Ru}(\text{NH}_3)_6^{3+}$  trapped inside the junction and could shift so significantly that the limiting currents were no longer observable in the potential range of mercury (Figure 4e).

Redox centers incorporated in molecular assemblies such as self-assembled monolayers and polymers have previously been shown to exhibit formal potentials that are shifted from their values in solution.<sup>45–49</sup> The work of Tsou and Anson, for example, showed that incorporation of  $\text{Ru}(\text{NH}_3)_6^{3+}$  into perfluorinated polycarboxylate coatings<sup>50</sup> in 0.2 M  $\text{CH}_3\text{COONa}$  supporting electrolyte solutions led to a negative shift of 162 mV in the formal potential.<sup>27</sup> They interpreted this shift in terms of two types of competing and opposing interactions: (i) a hydrophobic interaction between the fluorocarbon component of the polyelectrolyte and the  $\text{Ru}(\text{NH}_3)_6^{3+2+}$  couple that favors the less-charged, reduced  $\text{Ru}(\text{NH}_3)_6^{2+}$  species, and (ii) an electrostatic interaction with the hydrophilic carboxylate groups that favors the oxidized  $\text{Ru}(\text{NH}_3)_6^{3+}$  species. The hydrophobic and electrostatic interactions are expected to shift the formal potential to positive and negative values, respectively. The observation that the formal potential shifts toward negative potentials in our experiments suggests that the latter type of interaction (i.e., electrostatic stabilization of the ruthenium species) is dominant for the  $\text{Ru}(\text{NH}_3)_6^{3+2+}$  couple. In the  $\text{Hg}-\text{SC}_{10}\text{COO}^-/\text{Ru}(\text{NH}_3)_6^{3+2+}/\text{OOCC}_{10}\text{S}-\text{Hg}$  system, the formal potential (denoted as  $E_{1/2}$ ) of the ruthenium species shifts negatively from the value measured at an isolated SAM-coated mercury electrode. The ruthenium species could form (i) tight ion pairs with their counterions and/or (ii) electrostatic interactions with the carboxylate groups of the SAMs.

How could this increase in electrostatic interactions with increasing number of cycles in potential occur? A plausible

explanation is that it might arise by ejection of  $\text{Cl}^-$  from the junction (in order to maintain electroneutrality as  $\text{Ru}(\text{NH}_3)_6^{3+2+}(\text{Cl}^-)_{3/2}$  is converted to  $\text{Ru}(\text{NH}_3)_6^{3+2+}(\text{CO}_2^-)_x(\text{Cl}^-)_{3/2-x}$ ). The observation that the negative shift in  $E^\circ$  is accompanied by an increase in current and that repeated cycling of the potential is not always sufficient for these two parameters to change strongly suggests that another factor must also be operative. We propose that a decrease in the spacing between the electrodes must also occur. Two observations form the basis for this proposal. (i) The voltammetric responses for the  $\text{Ru}(\text{NH}_3)_6^{3+2+}$  couple at the generator electrode before and immediately after formation of the junction are essentially indistinguishable. This observation suggests that the environment experienced by the ruthenium ions inside the junction (at least during the first few potential cycles) is initially similar to that at a single, SAM-modified electrode in contact with bulk solution. For such an environment to exist inside the junction, the initial separation between the generator and collector electrodes must be sufficiently large to allow solvent and electrolyte to move into and out of the junction. (ii) With continued cycling,  $E_{1/2}$  shifts to negative potentials, and the currents in cyclic voltammetry increase at both the generator and collector electrodes. A decrease in the interelectrode distance would lead to an increase in currents, since the number of redox cycles per  $\text{Ru}(\text{NH}_3)_6^{3+2+}$  ion across the junction would increase. The negative shift in  $E_{1/2}$  on the other hand could be rationalized by an increase in electrostatic interactions between the ruthenium species with the carboxylate groups of the SAMs and/or with their counterions. While the formation of tight ion pairs between the ruthenium species and their counterions would be favored by a hydrophobic environment inside the junction, the decrease in interelectrode spacing leads rather to an increase in the concentration of the carboxylate groups and hence an increase in the hydrophilicity inside the junction. Therefore, we propose that  $E_{1/2}$  shifts negatively because of an increase in electrostatic interactions between the surface-immobilized  $\text{COO}^-$  groups and the  $\text{Ru}(\text{NH}_3)_6^{3+}$  couple.

The interelectrode spacing in principle could decrease by at least five different pathways: (i) loss of water and electrolyte from the junction, (ii) lateral expulsion of the SAMs from the mercury electrodes and formation of either low-density SAMs or SAMs containing more defects, (iii) tilting/compression of the SAMs, coupled with expulsion of electrolyte, due to electrostriction, (iv) tilting of the SAMs due to a change in the shape/area of the mercury drops, and (v) interpenetration of opposing SAMs. The loss of electrolyte solution, in particular the anions, from the junction would explain the observed negative shift for  $E_{1/2}$ . The proposal that the SAMs either tilt or compress with changes in applied potential<sup>28,22</sup> and/or shape/area<sup>15</sup> of the mercury-drop electrodes has precedents in the literature. The first proposal that SAMs of organothiols could tilt under the influence of electrostatic pressure for example was that of Majda et al.<sup>15</sup> In this study, experimental data involving capacitance, coulometric, and tunneling measurements led Majda to postulate that expansion of mercury-drop electrodes coated with alkanethiolate SAMs resulted in an increase in the tilt of the SAMs from their initial perpendicular orientation and hence a decrease in their geometric thickness. This proposal requires a lateral spreading of the SAM. In more recent studies (conducted in the absence of a solvent), Lindsay et al.<sup>28</sup> and Cahen et al.<sup>22</sup> invoked the compression and tilting of the SAMs under an applied electric field in order to explain the magnitude of their tunneling currents. In Lindsay’s study, the compression of the SAMs was proposed to occur during AFM-mediated electron transport mea-

(45) Rowe, G. K.; Creager, S. E. *Langmuir* **1991**, *7*, 2307–2312.  
 (46) Rowe, G. K.; Creager, S. E. *J. Phys. Chem.* **1994**, *98*, 5500–5507.  
 (47) De Long, H. C.; Donohue, J. J.; Buttry, D. A. *Langmuir* **1991**, *7*, 2196–2202.  
 (48) De Long, H. C.; Buttry, D. A. *Langmuir* **1992**, *8*, 2491–2496.  
 (49) Oyama, N.; Shimomura, T.; Shigehara, K.; Anson, F. C. *J. Electroanal. Chem. Interf. Electrochem.* **1980**, *112*, 271–280.  
 (50) This polymer is a derivative of Nafion; that is, it is a perfluoro polymer with side groups containing carboxylate substituents.

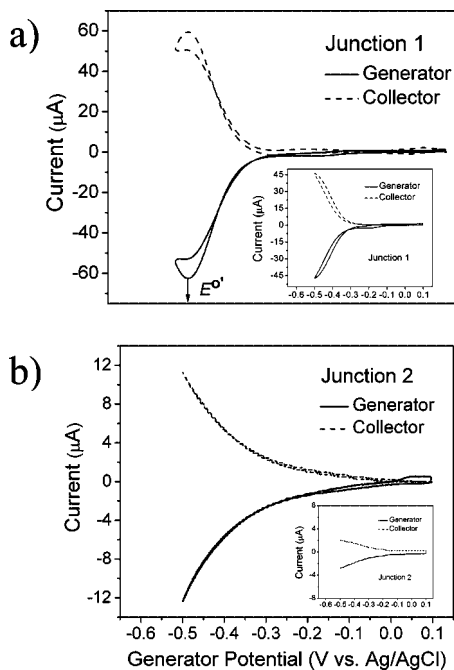


**Figure 5.** Generation-collection voltammograms obtained for Junction 1 (a) and Junction 2 (b) formed by assembling the  $\text{Hg}-\text{SC}_{10}\text{COO}^-/\text{Ru}(\text{NH}_3)_6^{3+/2+}/\text{OOCC}_{10}\text{S}-\text{Hg}$  junction in 1 mM  $\text{Ru}(\text{NH}_3)_6^{3+}$  in 0.1 M NaF at pH 9. In each case, the potentials of the generator and collector electrodes were cycled between +0.10 and -0.50 V with a 100-mV difference between them and a scan rate of 20 mV/s. Insets: the collector potential was held at +0.10 V, and the generator potential was cycled between +0.10 and -0.50 V at a scan rate of 50 mV/s. The area of the junction was ca. 0.79 mm<sup>2</sup>.

surements on  $\text{Au}-\text{S}(\text{CH}_2)_n\text{CH}_3/\text{Au}$  systems; in Cahen's study, the evidence suggested that short-chain alkanethiols ( $n < 12$ ) in mercury junctions of the type  $\text{Hg}-\text{S}(\text{CH}_2)_n\text{CH}_3/\text{SiO}_2/p\text{-Si}$  and  $\text{Hg}-\text{S}(\text{CH}_2)\text{CH}_3/p\text{-Si}-\text{H}$  tilted under electrostrictive pressure. These proposals may be correct but can only occur if the SAM spreads laterally (or has a high density of defects).

We propose that the interelectrode spacing in the  $\text{Hg}-\text{SC}_{10}\text{COO}^-/\text{Ru}(\text{NH}_3)_6^{3+/2+}/\text{OOCC}_{10}\text{S}-\text{Hg}$  junction also decreases as a result of (or perhaps is accompanied by) either interpenetration of the SAMs on the opposing mercury electrodes and/or formation of new defect sites in the SAMs. The experimental basis of this proposal is the observation that, after a junction had been cycled sufficiently to produce a steady-state voltammogram (e.g., Figure 4e), it was no longer stable to prolonged cycling of the potential. In fact, in all cases, such junctions persisted for only two to three cycles before the SAM-covered mercury-drop electrodes fused with one another and caused the junctions to short-circuit.

**Generation-Collection Experiment B<sup>Both</sup>. Scanning of the Potentials of Both Mercury Electrodes.** In this type of experiment, we scanned the potentials of both mercury electrodes while maintaining a constant difference in potential between them. Figure 5 shows representative steady-state current–potential curves for two different junctions (Junction 1 and Junction 2) when the potential difference between the mercury electrodes was fixed at 100 mV. The figure also shows (inset), for each junction, the corresponding current–potential curve when the potential of one mercury electrode was kept constant while that of the second electrode was varied (i.e., results of generation–collection experiment A<sup>Gen</sup>). Figure 5a shows that the generator (cathodic) and collector (anodic) currents of Junction 1 first

increase, reach a maximum at -473 mV, and then decrease as the potentials of both mercury electrodes are scanned with a 100-mV difference between them. The currents first increase due to conversion of Ru(III) to Ru(II) at the generator electrode and Ru(II) to Ru(III) at the collector electrode. The currents reach a maximum value when the average of the electrode potentials approach  $E^\circ$  for the  $\text{Ru}(\text{III}) \rightleftharpoons \text{Ru}(\text{II})$  interconversion. When the potentials of both mercury electrodes are more negative than  $E^\circ$ , the currents decrease because the concentration of Ru(III) decreases at both electrodes. The observation of a peak at -473 mV therefore confirms that  $E^\circ$  in the environment of the junction can be significantly shifted from that observed for  $\text{Ru}(\text{NH}_3)_6^{3+/2+}$  in solution.

Figure 5b shows the results obtained for Junction 2. In this case, the generator (cathodic) and collector (anodic) currents of Junction 2 do not increase and then decrease as the potentials of both mercury electrodes are scanned with a constant 100-mV difference between them. Instead, the currents increase smoothly as the potentials are scanned to -500 mV. This result demonstrates that  $E_{1/2}$  can be so shifted negatively that it no longer falls within the potential window of mercury.

**Stability of the  $\text{Hg}-\text{SC}_{10}\text{COO}^-/\text{Ru}(\text{NH}_3)_6^{3+/2+}/\text{OOCC}_{10}\text{S}-\text{Hg}$  Junctions and the Reproducibility of Their Electrochemical Behavior.** We assembled a total of 39 junctions in this study: 14 shorted within the first few potential scans while 25 were stable over 10–15 scans. Of these more stable junctions, 10 persisted for five or more minutes of continued cycling (a total of about five scans) but shorted before the generator current increased significantly or became sigmoidal. The remaining 15 (or 38% of the junctions examined) produced steady-state voltammograms, but these steady-state systems also typically persisted for only one to two scans before shorting. Thus this system, as least as we were operating it, never seems to reach a state where it shows long-term stability.

In general, the number of potential cycles and lengths of time under applied potential required for the currents to reach steady state fell in the ranges of 5–10 cycles and 10–15 min, respectively. The shape of the steady-state voltammograms and the location of  $E_{1/2}$  however differed for different junctions, depending on the extent to which the curves shifted to negative potentials. Thus, for some junctions, a sigmoidal current response with well-defined limiting currents could be observed; the current–potential curves of other junctions were so shifted that neither the limiting currents nor the values of  $E_{1/2}$  could be observed within the potential range of mercury (Figure 5b). For comparison, the limiting currents that could be observed ranged from 6 to 40 μA whereas the maximum currents observed at -500 mV in junctions showing no limiting currents in the potential range of mercury ranged from 6 to 60 μA.

For a given area of contact between the two SAM-covered mercury drops, the electrochemical behavior of the junction varied in a systematic manner as it progressed toward steady state. In all cases, increasing the number of cyclic potential sweeps and the area/distortion of the mercury drops resulted in (i) an increase in the amplitude of the junction current, (ii) an increase in the collection efficiency, and (iii) a more negative shift of  $E_{1/2}$ . The variation of values of  $E_{1/2}$  and the limiting currents from one junction to another seem to reflect a sensitivity to many factors, not all of which we can control. For example, both values are dependent on the interelectrode spacing and the organization of the SAMs. The SAMs do not have a static structure that is uniquely determined by the process used for self-assembly; rather, the monolayers probably rearrange upon

either expansion of the mercury drops or forming the contact and perhaps also under electrostrictive pressure.<sup>17</sup> Unless all such factors can be accurately reproduced during assembly and electrochemical measurements, the current response to applied potential may vary from junction to junction.

**Mechanistic Implications.** Mechanistically, charge transport in macromolecular assemblies containing redox centers may occur by physical diffusion of the redox centers between interfaces and/or by hopping of electrons between adjacent oxidized and reduced sites; the relative rates of these processes will depend on the spatial arrangement of the redox centers in the supramolecular and macroscopic assemblies, on the viscosity of the medium, on the rate constant for intermolecular tunneling, on the composition of the medium, and on other factors. Equation 1 shows the apparent diffusion coefficient,  $D_{\text{ap}}$  (cm<sup>2</sup>/s), resulting from a combination of physical displacement and electron hopping; here, the first term  $D_{\text{phys}}$  (cm<sup>2</sup>/s) is the diffusion coefficient for physical displacement of the redox molecules, and the second term represents the diffusion coefficient of charge due to electron hopping between two ruthenium centers.<sup>7,8,51</sup> In the second term of eq 1,  $k_{\text{ex}}$  (cm<sup>3</sup>/mol·s) is the bimolecular rate constant for electron self-exchange,  $C$  (M) is the total concentration of redox species, and  $\delta$  (cm) is the electron-transfer contact distance.

$$D_{\text{ap}} = D_{\text{phys}} + \frac{k_{\text{ex}} \delta^2 C}{6} \quad (1)$$

The experimental results indicate that, immediately after the formation of the junction and during the first few potential cycles, charge transport across the junction is dominated by a process involving molecular diffusion, most plausibly by redox shuttling in which the Ru(NH<sub>3</sub>)<sub>6</sub><sup>3+/2+</sup> couple diffuses back and forth between the two electrodes. This mechanism is supported by two types of evidence: (i) both the generator and collector electrodes exhibit electrochemical reactions at the same potential as soluble, freely diffusing Ru(NH<sub>3</sub>)<sub>6</sub><sup>3+</sup>, and (ii) the current at the collector electrode is smaller than that at the generator and can be almost negligible.

After the junction has been subjected to repeated cycling (typically at least five to six cycles), the results suggest a decrease in the interelectrode spacing. Such a decrease could lead to an increase of the viscosity and to a decreased of the mobility of the Ru(NH<sub>3</sub>)<sub>6</sub><sup>3+/2+</sup> when associated with the COO<sup>-</sup> charged groups.<sup>52</sup> Under these extreme conditions, it may be possible that a different mechanism begins to dominate the electrochemical behavior of the Hg–SAM//Ru(NH<sub>3</sub>)<sub>6</sub><sup>3+/2+</sup>//SAM–Hg junction. If the concentrations of the ruthenium species inside the junction for example become so low such that they become a monolayer or a submonolayer, then charge transport across the junction would involve electron donation from the generator electrode to the Ru(III) species, followed by electron donation from the newly generated Ru(II) species to the collector electrode. According to this proposed mechanism, the collection efficiency (i.e., the ratio of the currents at the generator and collector electrodes) would be expected to be equal to 1. However, since the ratio of the currents at the generator and collector electrodes approaches but never quite reaches 1 in our junction (as mentioned above), the possibility of this mechanism being operative is unlikely. Another piece

of evidence that would rule out the existence of a monolayer or submonolayer of ruthenium species comes from a study of a junction we reported in 2004.<sup>11</sup> In this study, the junction consisted of two liquid mercury-drop electrodes whose surfaces were covered by SAMs terminated with covalently attached Ru(II) centers. We found that, when one electrode was covered with a Ru-terminated SAM and the other electrode was covered with a COO<sup>-</sup>-terminated SAM, charge transport across the junction was essentially negligible (i.e., when a junction has a monolayer or a submonolayer of ruthenium species, a two-step tunneling mechanism was not observed).

A number of studies have concluded that the contribution of the electron-hopping term to charge transport is very small in electrochemical processes occurring in solution.<sup>53–55</sup> This process can however become important when the magnitude of  $D_{\text{phys}}$  become small.<sup>56–58</sup> Small values of  $D_{\text{phys}}$  (and  $D_{\text{ap}}$ ) have been reported in a number of experimental studies of charge and mass transport in polymer-coated electrodes, where both electron hopping and physical diffusion contributed to the overall charge transport process.<sup>56,59</sup>

We propose that the increase in medium viscosity and in immobilization of Ru(NH<sub>3</sub>)<sub>6</sub><sup>3+/2+</sup> inside the Hg–SC<sub>10</sub>COO<sup>-</sup>//Ru(NH<sub>3</sub>)<sub>6</sub><sup>3+/2+</sup>//OOCC<sub>10</sub>S–Hg junction at very small inter-electrode spacing would likely be accompanied by a significant decrease in  $D_{\text{phys}}$  and hence  $D_{\text{ap}}$ . Under these circumstances, if  $D_{\text{phys}}$  decreases sufficiently, we cannot exclude a contribution from electron hopping to the overall charge transport.<sup>56,59</sup>

## Conclusions

By using two mercury-drop electrodes modified with COO<sup>-</sup>-terminated SAMs, it is possible to produce a metal–molecules–metal junction that allows redox centers dissolved in solution to be incorporated between the two metal electrodes. The COO<sup>-</sup>-terminated SAMs can act both as spacers between the electrodes that prevent fusion and shorting of the electrodes and as permeable layers that allow the redox centers to have easy access to the surface of the electrodes. Conventional electrochemical techniques demonstrate that the current flowing through the Hg–SC<sub>10</sub>COO<sup>-</sup>//Ru(NH<sub>3</sub>)<sub>6</sub><sup>3+/2+</sup>//OOCC<sub>10</sub>S–Hg junction can be switched from “off” to “on” by controlling the potentials of the electrodes with respect to the formal potential of the redox couple. The charge flows through the junction only when the potentials of the mercury electrodes are adjusted so that one

(53) Dahms, H. *J. Phys. Chem.* **1968**, *72*, 362–364.  
 (54) Ruff, I.; Friedrich, V. *J. Phys. Chem.* **1971**, *75*, 3297–3302.  
 (55) Ruff, I.; Friedrich, V. J.; Demeter, K.; Csillag, K. *J. Phys. Chem.* **1971**, *75*, 3303–3309.  
 (56) Buttry, D. A.; Anson, F. C. *J. Electroanal. Chem.* **1981**, *130*, 333–338.  
 (57) Facci, J.; Murray, R. W. *J. Phys. Chem.* **1981**, *85*, 2870–2873.  
 (58) Previously, Bard and coworkers demonstrated that Nafion films incorporating either Cp<sub>2</sub>FeTMA<sup>+</sup>, Ru(bpy)<sub>3</sub><sup>2+</sup>, or Os(bpy)<sub>3</sub><sup>2+</sup> conducted by a mechanism involving both electron hopping and physical diffusion. The relative contributions of electron hopping and physical diffusion to the overall charge transport process depended on the nature of the incorporated electroactive ion. For Cp<sub>2</sub>FeTMA<sup>+</sup>, the contribution of the electron-hopping term was less than 6%. In this case, Bard and coworkers concluded that, although both electron hopping and physical diffusion occurred, the latter was rate-limiting. For Ru(bpy)<sub>3</sub><sup>2+</sup>, the contribution of the electron-hopping term was 93%, and for Os(bpy)<sub>3</sub><sup>2+</sup>, it was 57%. For all three electroactive ions,  $D_{\text{ap}}$ ,  $D_{\text{phys}}$ , and  $k_{\text{ex}} \delta^2 C / 6$  were all in the 10<sup>-10</sup> cm<sup>2</sup> s<sup>-1</sup> range. Anson and coworkers reached a similar conclusion in their study of the behavior of Ru(bpy)<sub>3</sub><sup>2+</sup> and Co(bpy)<sub>3</sub><sup>2+</sup> in Nafion films. They too found electron hopping to be of major importance for the Ru species.  
 (59) White, H. S.; Leddy, J.; Bard, A. J. *J. Am. Chem. Soc.* **1982**, *104*, 4811–4817.

(51) Anson, F. C.; Blauch, D. N.; Saveant, J.-M.; Shu, C.-F. *J. Am. Chem. Soc.* **1991**, *113*, 1922–1932.  
 (52) Porter, J. D.; Zinn, A. S. *J. Phys. Chem.* **1993**, *97*, 1190–1203.

electrode donates electrons to the  $\text{Ru}(\text{NH}_3)_6^{3+}$  centers and the other electrode accepts them from the  $\text{Ru}(\text{NH}_3)_6^{2+}$  centers. The current flow is mediated by the ruthenium centers inside the junction and occurs via a redox cycling mechanism during the initial potential cycles.

The current increases by more than an order of magnitude and is accompanied by a large negative shift in the formal potential ( $\Delta E^\circ > 262$  mV) for the reduction of  $\text{Ru}(\text{NH}_3)_6^{3+}$  on repeated cycling of the potential across the junction and/or by decreasing the size of the gap between the two syringes supporting the mercury electrodes followed by repetitive cycling of the potential. We interpret the marked increase in current to be a result of a decrease in the gap between the mercury electrodes. We attribute the shift toward negative potential on repeated cycles to extrusion of the electrolyte anions from the junction and to association of the  $\text{Ru}(\text{NH}_3)_6^{3+/2+}$  ions with the  $\text{COO}^-$  group in the SAMs.

While it is clear that the mechanism responsible for the currents measured when the  $\text{Hg}-\text{SC}_{10}\text{COO}^-/\text{Ru}(\text{NH}_3)_6^{3+/2+}/\text{OOC-C}_{10}\text{S-Hg}$  junction is first assembled is redox cycling, we considered the possibility that a “hopping of charges” between ruthenium centers in the junction might become competitive with redox cycling when the electrode separation is at its most narrow. We cannot carry out definitive experiments because the operating lifetime of the junctions is short, the concentration of the ruthenium ions changes during measurement (and is probably never well-defined), the diffusion constant of the  $\text{Ru}(\text{NH}_3)_6^{3+/2+}$  couple also changes with changing conditions in the junction, and the interelectrode separation changes.

These results indicate that junctions of the type  $\text{Hg-SAM//R//SAM-Hg}$  are relatively tractable subjects for experimental study of charge transport. They also provide an easy, new methodology to fabricate junctions, in which the charge transport is mediated by charged redox centers incorporated into the solution between the electrodes. These new  $\text{Hg-SAM//R//SAM-Hg}$  junctions have several useful attributes: (i) While the fabrication of closely spaced ( $<1\ \mu\text{m}$ ) electrodes required for efficient redox cycling to occur can require sophisticated fabrication techniques, junctions of the type  $\text{Hg-SAM//R//SAM-Hg}$  are both easy and inexpensive to assemble and give small ( $<10\ \text{nm}$ ) interelectrode separations. (ii) The redox centers can be incorporated by ion exchange into metal-SAM//SAM-metal junctions without difficult chemical synthesis of thiol-functionalized redox organic/organometallic species. (iii) Both the area and electrical properties of these types of junctions can be easily modified. For example, the area may be modified by changing the mercury drop sizes and/or by decreasing the gap between the two syringes supporting the mercury electrodes. Changing the electrical properties may be achieved by changing the nature of the redox centers.

These junctions also suffer from a number of limitations however. Most importantly, they have short operating lifetimes. Their behavior changes with time as the electrolyte layer thins. The contact area between the liquid mercury electrodes is difficult to control, and this difficulty is reflected by significant variability (up to 30%) in current from junction to junction.

| electroactive ion              | $D_{\text{ap}}\ (\times 10^{-10}\ \text{cm}^2\ \text{s}^{-1})$ | $D_{\text{phys}}\ (\times 10^{-10}\ \text{cm}^2\ \text{s}^{-1})$ | electron hopping<br>( $\times 10^{-10}\ \text{cm}^2\ \text{s}^{-1}$ ) | electron-hopping contribution |
|--------------------------------|--|--|---|-------------------------------|
| $\text{Cp}_2\text{FeTMA}^+$    | 1.7  | 1.6–1.8  | 0.1   | <6%                           |
| $\text{Ru}(\text{bpy})_3^{2+}$ | 4  | 0.2–0.3  | 3.7   | 93%                           |
| $\text{Os}(\text{bpy})_3^{2+}$ | 0.7  | 0.2–0.3  | 0.4–0.5   | 57%                           |

Mercury is toxic and environmentally unfriendly. The potential window of mercury is also quite narrow (ca.  $-0.6$  to  $+0.2\ \text{V}$  vs  $\text{Ag}/\text{AgCl}$ ); this limited window reduces the choice of redox centers that can be studied inside the junction.

Despite these limitations, we believe that the  $\text{Hg-SAM//R//SAM-Hg}$  junctions, like our previously reported junctions of the form  $\text{Hg-SAM-R//R-SAM-Hg}$  (in which the redox sites are covalently attached to the two SAMs), are a convenient and versatile system for exploration, screening, and mechanistic examination of electron-transfer processes mediated by redox centers. They also may be used to compare current flow when the redox centers are incorporated into the junction via different type of interactions. In fact, our previous work on the  $\text{Hg-SAM-R//R-SAM-Hg}$  junction showed it to conduct via an electron-hopping mechanism between adjacent oxidized and reduced sites.<sup>11</sup> The  $\text{Hg-SAM//R//SAM-Hg}$  junction described in this paper, however, conducts primarily by a redox-cycling mechanism.

In the study of charge transport across two electrodes, the energy gap between the Fermi levels of the metal electrodes and the energy states of the molecules is often difficult to control. In electrochemical junctions, using an external reference electrode allows the potential of the mercury electrodes to be controlled with respect to the redox state of the incorporated molecules. These electrochemical junctions thus make it possible not only to control the current flow across the junction but also to predict the potential value at which current onset occurs. In both the  $\text{Hg-SAM//R//SAM-Hg}$  and  $\text{Hg-SAM-R//R-SAM-Hg}$  junctions, this control makes it possible to switch current from an “off” to an “on” signal at the formal potential of the redox couple that is incorporated into the junction.

The use of molecules with multiple redox states and the possibility of addressing each redox state via the reference electrode represent a powerful approach toward thin-film devices of well-defined electrical behavior. The  $\text{Hg}$ -based electrochemical junctions are convenient prototype systems that may provide important information (e.g., effects of confined space on charge transport mechanism, on mass transport parameters as diffusion and ion exchange, and on charge interactions) for the field of organic electronics.

**Acknowledgment.** The support of NSF (Award No. CHE-0518055), CNR (Italy, Grant G5RD-CT-2002-00776 MWFM), the European Union (Grant IST-2001-35503 LIMM), NSERC (in the form of a postdoctoral fellowship to E.T.), and MURST is gratefully acknowledged. We thank Irina Gitlin, Logan McCarty, Roman Boulatov, and Rosaria Ferrigno for helpful discussions, and in particular, William Reus for the graphic illustration shown in the Table of Contents.

JA804075Y